

# Substrate-induced band gap opening in epitaxial graphene

S.Y. Zhou,<sup>1,2</sup> G.-H. Gweon,<sup>1,\*</sup> A.V. Fedorov,<sup>3</sup> P.N. First,<sup>4</sup> W.A. de Heer,<sup>4</sup>

D.-H. Lee,<sup>1</sup> F. Guinea,<sup>5</sup> A.H. Castro Neto,<sup>6</sup> and A. Lanzara<sup>1,2</sup>

<sup>1</sup>*Department of Physics, University of California, Berkeley, CA 94720, USA*

<sup>2</sup>*Materials Sciences Division, Lawrence Berkeley*

*National Laboratory, Berkeley, CA 94720, USA*

<sup>3</sup>*Advanced Light Source, Lawrence Berkeley National*

*Laboratory, Berkeley, California 94720, USA*

<sup>4</sup>*School of Physics, Georgia Institute of Technology, Atlanta, GA 30332-0430*

<sup>5</sup>*Instituto de Ciencia de Materiales de Madrid,*

*CSIC, Cantoblanco, E-28049 Madrid, Spain.*

<sup>6</sup>*Department of Physics, Boston University,*

*590 Commonwealth Avenue, Boston, MA 02215, USA*

(Dated: November 18, 2007)

---

\*Present address: Department of Physics, University of California, Santa Cruz, California 95064, USA

Graphene has shown great application potentials as the host material for next generation electronic devices. However, despite its intriguing properties, one of the biggest hurdles for graphene to be useful as an electronic material is its lacking of an energy gap in the electronic spectra. This, for example, prevents the use of graphene in making transistors. Although several proposals have been made to open a gap in graphene's electronic spectra, they all require complex engineering of the graphene layer. Here we show that when graphene is epitaxially grown on the SiC substrate, a gap of  $\approx 0.26$  eV is produced. This gap decreases as the sample thickness increases and eventually approaches zero when the number of layers exceeds four. We propose that the origin of this gap is the breaking of sublattice symmetry owing to the graphene-substrate interaction. We believe our results highlight a promising direction for band gap engineering of graphene.

Graphene, an atomically thin layer of carbon atoms arranged in a honeycomb lattice, has attracted a lot of research interest because of its intriguing physics as well its application potential [1–4]. In particular, the extremely high mobility and the easy control of charge carriers by applying a gate voltage have made graphene a promising material for next generation electronics with properties that may exceed those of conventional semiconductors. In single layer graphene, the unit cell consists of two carbon atoms - the A and B sublattices (Fig.1a). The band structure of graphene exhibits two bands intersecting at two inequivalent points K and K' in the reciprocal space (Fig.1a). Near these points, the electronic dispersion resembles that of relativistic Dirac electrons. For this reason, K and K' are commonly referred to as the “Dirac points”. As the valence and conduction bands are degenerate at the Dirac points, graphene is a zero gap semiconductor, and how a gap can be induced is crucial for its application in making devices. There are two ways to lift the degeneracy of the two bands at the Dirac points. One is to hybridize the electronic states at K and K', which requires breaking of the translational symmetry [5]. The other is to break the equivalence between the A and B sublattice, which does not require any translation symmetry breaking [6–12]. To induce these perturbations, various graphene super-structures, such as graphene quantum dots [6], graphene ribbons [7–10], and devices based on the combination of single and bilayer graphene regions [11, 13, 14] have been proposed. Here we show that a gap can be induced in a much easier and reproducible way in epitaxial graphene on a SiC substrate.

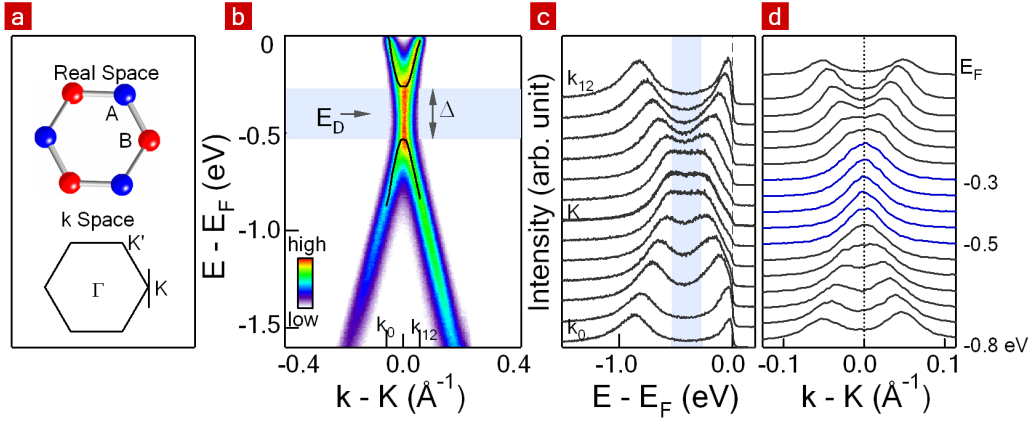


FIG. 1: **Observation of the gap opening in single layer graphene at the K point.** (a) Structure of graphene in the real and momentum space. (b) ARPES intensity map taken along the black line in the inset of panel (a). The dispersions (black lines) are extracted from the EDC peak positions shown in panel (c). (c) EDCs taken near the K point from  $k_0$  to  $k_{12}$  as indicated at the bottom of panel (b). (d) MDCs from  $E_F$  to -0.8 eV. The blue lines are inside the gap region, where the peaks are non-dispersive.

As we shall discuss, the interaction between the graphene layer and the substrate will break the A and B sublattice symmetry, which opens up a band gap.

Figure 1 shows ARPES data taken on single layer graphene for a line through one of the Dirac points, the K point. Panel (b) shows the photoelectron intensity as a function of energy and the momentum along the black line through K in panel (a). The black curves mark the location of peak positions in the energy distribution curves (EDCs). Following the maximum in the intensity map, an upward-dispersing and a downward-dispersing cone are clearly observed. This agrees with the expected conical dispersion of relativistic electrons near the Dirac points. From the mid-point between the minimum of the conduction band and the maximum of the valence band, we deduce that,  $E_D$ , the energy of the expected Dirac point, is about 0.4 eV below the Fermi energy ( $E_F$ ). This is in contrast to what is expected for the undoped graphene where  $E_D = E_F$ , showing that the as-grown graphene is electron doped [4, 15]. Surprisingly, the dispersion at  $E_D$ , i.e. the intersection of the cones, is not characterized by a single point as expected for monolayer graphene. Instead, the valence and conduction bands are separated by a finite energy even at the K point and a gap-like feature is observed. This directly follows from the analysis of the EDCs shown in panel (c)

and the momentum distribution curves (MDCs) in panel (d). Near the K point, the EDCs show always *two peaks* with the minimum energy separation, or the gap, being realized at K. From this we deduce a gap of  $\approx 0.26$  eV. The MDC peaks are non-dispersive within the same energy window, 0.26 eV around  $E_D$  (blue lines in panel d). Clearly away from this region, the MDC peaks start dispersing again, in agreement with a conical dispersion.

A peculiar feature of this gap is that there is non-zero intensity around  $E_D$  (panel b) between the valence and conduction bands. Does this mean that there is no gap at the K point? If we consider cuts away from the K point (see Fig.S3(a) in supplementary information), based on the conical dispersion of Dirac fermions, a large gap is expected. However, even this large gap is characterized by a finite intensity. Therefore we conclude that the non-zero intensity does not mean absence of a gap and in fact there is a gap at the K point. The remaining question is what is causing this finite intensity inside the gap. This is very likely the result of the broad EDC peaks (Fig. 1(c)) which cause an overlap of the intensity tails from the top of the valence band and the bottom of the conduction band. Although at this stage it is not clear why the EDC peaks are so broad, possible causes may be a self energy effect or distribution of gaps. Finally regardless of the origin, what the large EDC width implies in terms of actual device application remains to be seen in the future. One should note that ARPES lifetime determined as the inverse line width tends to underestimate the transport lifetime by as much as two orders of magnitude [16], and that in general one would expect a sharpening up of peaks as they are brought to the Fermi level, as would happen in device applications.

We note that similar data have been reported recently and discussed in terms of electron-plasmon interaction [17]. This interpretation is based on the departure of the dispersion from the anticipated behavior near  $E_D$  and the observation of an anomalous upturn of the MDC width near  $E_D$ . However, these are *not* unique features of the K point and they occur every time a gap is present in the spectra. To discuss the MDC width near the top or bottom of the band in terms of many-body interactions is misleading, as this anomalous upturn of the width often occurs in ARPES near the bottom or the top of a band and is thus an artifact of the MDC analysis. This is one of the reasons why EDC analysis is more appropriate to extract both the dispersion and the life time in this context. Finally, since  $E_D$  is not at the Fermi energy, within the explanation proposed in Ref.17 it requires a coincidence for the plasmon feature to center around  $E_D$ . In addition, it is quite unlikely that the plasmon

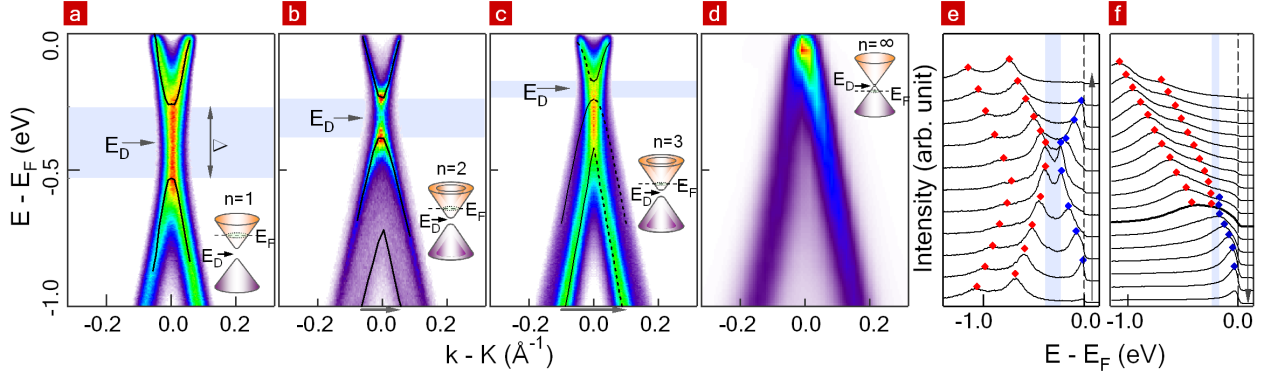


FIG. 2: **Decrease of the gap size as the sample becomes thicker.** (a-d) ARPES intensity maps taken on single layer graphene on 6H-SiC, bilayer graphene on 4H-SiC, trilayer graphene on 6H-SiC and graphite respectively. Data were taken along the black line in the inset of Fig.1(a) except panel (c), which was measured along  $\Gamma K$  direction and symmetrized with respect to the K point to remove the strong intensity asymmetry induced by dipole matrix element [33]. (e, f) EDCs taken from the raw data (without symmetrization) for momentum regions labeled by the arrows at the bottom of panels (b) and (c).

energy changes by a factor of two from the single layer to the bilayer graphene, where a similar tail is also observed.

Figures 2(a-c) show how the gap and the distance between  $E_D$  and  $E_F$  change as the graphene sample thickness varies. Panels (b) and (c) show the ARPES data for bilayer and trilayer graphene samples. Again the dispersions extracted from the EDCs (panels (e) and (f)) are plotted. In these two panels, two distinct cones can be identified for  $E < E_D$ . This is attributed to the splitting of the  $\pi$  bands induced by the interlayer coupling, similar to the  $\approx 0.7$  eV splitting observed in bulk graphite in the  $k_z=0$  plane [18, 19]. The absence of the  $\pi$  band splitting in panel (a) and the increase of the splitting from panel (b) to panel (c) is also a consistent check for the sample thickness determined by other methods [15, 20]. Panel (d) shows the ARPES data taken along a line through the H point in graphite, where the dispersion resembles that of graphene through K [18]. Data shown in panels (a-d) allow us to determine how the electronic structure near K point varies as the sample thickness increases. First of all, as the sample thickness increases,  $E_D$  shifts toward  $E_F$ . From single layer to trilayer graphene,  $E_D$  (marked by arrows in panels (a-c)) shifts from -0.4 eV to -0.29

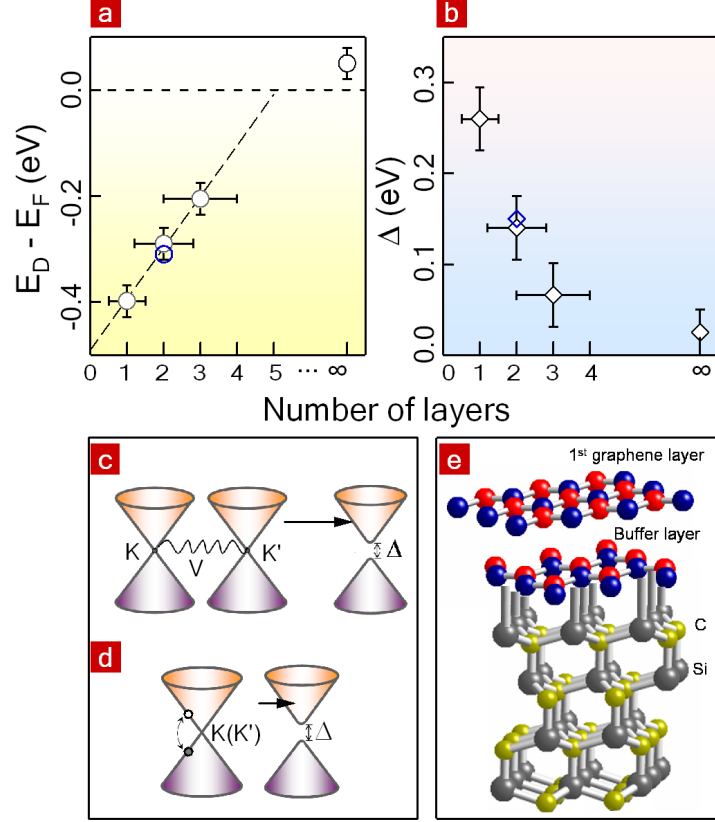


FIG. 3: **Thickness dependence of  $E_D$  and  $\Delta$ .** (a,b)  $E_D$  and  $\Delta$  as a function of sample thickness, for epitaxial graphene on 6H-SiC (black) and on 4H-SiC (blue). The error bar for the sample thickness was taken from the XPS measurements [15]. For graphite,  $E_D$  is extrapolated from the dispersions at  $k_z \approx \pi/c$  [18], and the gap is estimated from band structure calculation [21, 22]. (c, d) Two possible mechanisms to open up a gap at the Dirac point. (e) Schematic drawing to show the inequivalent potentials on the A (blue) and B (red) sublattices induced by the interface.

eV then to -0.2 eV. For graphite,  $E_D$  has been estimated to be at  $\approx 0.05$  eV above  $E_F$  [18]. More importantly, as the sample becomes thicker, the gap (labeled by light blue shaded area in panels (a-c)) decreases rapidly. From single layer to trilayer graphene, the gap decreases from 0.26 eV to 0.14 eV then to 0.066 eV. For graphite, since the Dirac point energy is above  $E_F$  [18], whether there is a gap or not cannot be directly addressed by ARPES. However, from band structure calculation, it is expected that the gap at the H point is  $\approx 0.008$  eV [21, 22], which is almost negligible.

Figures 3(a-b) summarize the evolution of the Dirac point energy  $E_D$  and the gap  $\Delta$  for various sample thickness. The layer dependence of both quantities suggests that, beyond 5 layers, epitaxial graphene behaves as bulk graphite [18]. The shift of  $E_D$  in panel (a) is most likely due to the electric field and surface charges present at the graphene-(n-SiC) interface [20]. We have also measured a bilayer graphene sample on a more insulating 4H-SiC substrate (Fig.2(b)) with resistivity of  $10^5 \Omega/\text{cm}$  compared to  $0.2 \Omega/\text{cm}$  in 6H-SiC. In both cases, the Dirac point energy appears to be shifted by a similar amount below  $E_F$ , suggesting that the doping is most likely associated with the surface charges at the interface, rather than the carrier concentration of the substrate. This effect should decrease as the sample becomes thicker, because the surface layer probed by ARPES is farther away from the interface as the thickness increases. Also, the strong dependence of  $E_D$  on sample thickness is a direct manifestation of the short interlayer screening length ( $\approx 5$  layers [23]) of graphene. This result shows that the sample thickness is an effective way of controlling doping in epitaxial graphene. Panel(b) shows the dependence of the gap on the sample thickness. A gap in bilayer graphene has been reported and attributed to the different potentials in the two graphene layers induced by doping or electric field [13, 14, 24]. While this could contribute to the gap in bilayer and even trilayer graphene, it certainly is not the reason for the gap in the single layer graphene.

In the following, we discuss two possible scenarios and we propose that the gaps in single, double and triple layer graphene are results of symmetry breaking due to the substrate. As discussed in the introduction, there are two ways to open up energy gaps at K and K'. The scenario that invokes the inter-Dirac-point hybridization (Fig.3c) requires translation symmetry breaking. The two known reconstructions on epitaxial graphene,  $6\times 6$  and  $(6\sqrt{3}\times 6\sqrt{3})R30^\circ$  [25] are obvious candidates for the source of this symmetry breaking. However, in order to mix K and K', a large scattering wave vector is required. This is much longer than the reciprocal lattice vectors of both reconstructions mentioned above. High ordering process involving consecutive small scattering wave vectors will be weak in general. Another source of inter-Dirac-point scattering is impurity scattering, which, as recently shown, can mix the wave functions at the two K points [26, 27]. This however would give rise to a gap that strongly depends on the impurity concentration, in contrast to our finding. The gap is in fact the same in all the samples that we have studied, prepared under different conditions (with and without hydrogen etching of the SiC substrate) and on differently

doped substrates, insulating vs slightly electron doped substrate.

In our opinion, the more likely scenario is the breaking of the A, B sublattice symmetry. This leads to the rehybridization of the valence and conduction band states associated with the same Dirac point (Fig.3d), resulting in a gap at all the K and K' points. A necessary prediction of this scenario is the breaking of the six fold rotational symmetry of graphene near the Dirac point energy. For energy well above and/or below  $E_D$ , the symmetry is restored. For bilayer and trilayer graphene, the breaking of the A, B sublattice equivalence can be a direct consequence of the the AB stacking between different layers. Indeed, topographic Scanning Tunneling Microscopy (STM) images for bilayer graphene have clearly shown inequivalent A and B sublattices [26, 28, 29], similar to what has been observed for graphite [30]. This simply derives from the fact that one sublattice has carbon atoms directly below it while the other does not. Naively it seems that this explanation will not work for single layer graphene. However, it is known that for epitaxially grown graphene, a buffer layer (Fig.3e) exists [31, 32]. ARPES study of the buffer layer has shown practically the same  $\sigma$  bands as graphene while very different  $\pi$  bands [32]. This is because the  $\pi$  orbitals have hybridized with the dangling bonds from the substrate. The fact that the  $\sigma$  bands are unchanged suggests that, like graphene, the carbon atoms in the buffer layer have also the honeycomb arrangement with similar bond length. Consequently, although the buffer layer is electronically inactive (absence of  $\pi$  orbitals) [32], structurally it can break the A, B sublattice symmetry when a single layer of graphene grows upon it (Fig.3e). This is particularly so in view of the small layer separation of  $\approx 2 \text{ \AA}$  [31] and the AB stacking usually expected for very thin graphene samples.

For the single and bilayer graphene, we use a tight binding model with symmetry breaking on the A and B sublattices to fit the symmetry breaking parameters to the observed energy gap (see supplementary information for the Bloch Hamiltonian). By fitting the dispersion, the symmetry breaking parameter in single layer graphene, defined as half of the difference between the substrate potentials on the A and B sublattices, is determined to be  $m \approx 0.13 \text{ eV}$ . In bilayer graphene, the symmetry breaking parameters in the top and bottom layers are  $m_1 \approx 0.49 \text{ eV}$ ,  $m_2 \approx -0.21 \text{ eV}$  respectively. The magnitude of the symmetry breaking parameter is much bigger in the bottom graphene layer than that in single layer graphene, because it is sandwiched between the buffer layer and the top graphene layer. The reason for  $m_2$  to have the opposite sign is because of the AB stacking. This cancels part of the



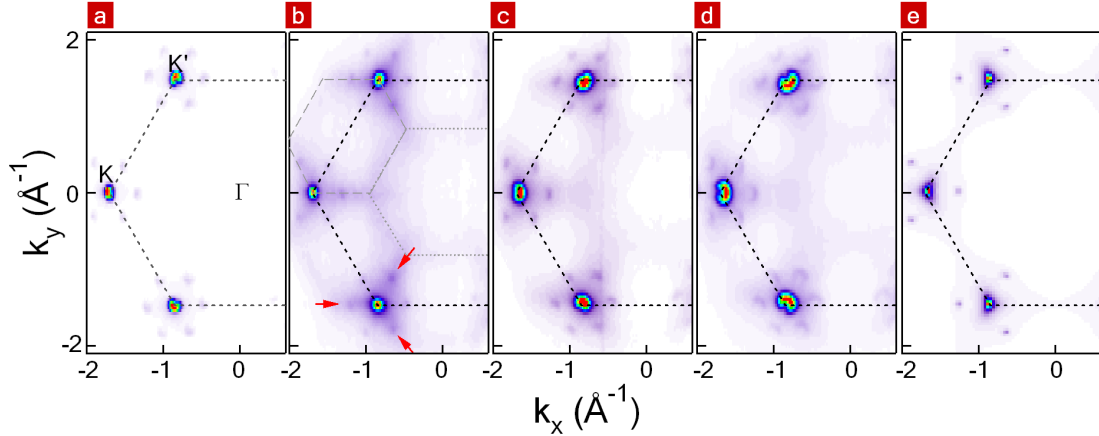


FIG. 4: **Breaking of the six fold symmetry in the intensity map near  $E_D$ .** (a-d) ARPES intensity maps taken on single layer graphene at  $E_F$ ,  $E_D$ ,  $-0.8$  eV and  $-1.0$  eV respectively. Near  $E_D$  (panel b), the intensity of the six replicas near K shows breaking of six fold symmetry. Note that to enhance the additional feature around  $E_D$ , the color scale is saturated for the dominant features near K and the replicas. (e) ARPES intensity map of the calculated spectral function at  $E_D$  in the presence of symmetry breaking on the two carbon sublattices.

effect in the bilayer graphene and decreases the gap. Therefore, for AB stacking graphene, the eigen functions average out for many layers, and the gap decreases rapidly.

Figure 4 shows additional support for the A, B sublattice symmetry breaking. Panels (a-d) show intensity maps taken on single layer graphene as a function of  $k_x$  and  $k_y$  at  $E_F$ ,  $-0.4$ ,  $-0.8$  eV and  $-1.0$  eV respectively. The dominant features in these panels are the small pockets centered at the six corners of the Brillouin zone. Interestingly, around each corner, there are six faint replicas forming a smaller hexagon. The intensity associated with them is  $\approx 4\%$  of the main intensity. Closer inspection shows that the vectors connecting the center of the small hexagon to its six corners are nearly the same as the second shortest reciprocal lattice vectors of the  $(6\sqrt{3} \times 6\sqrt{3})R30^\circ$  [15, 20] observed in low energy electron diffraction LEED [15, 20]. As  $E_D$  is approached, three among the six faint replicas become more intense (pointed by red arrows in Fig.4(b)). This suggests the breaking of the six fold rotational symmetry of graphene down to three fold, and is consistent with the notion of A and B sublattices being inequivalent. In Fig.4(e), we use a tight binding model to compute the intensity of the replicas at  $E_D$ . The potential modulation imposed by the  $(6\sqrt{3} \times 6\sqrt{3})R30^\circ$  reconstruction has been added as a perturbation to the Hamiltonian, and the sublattice

symmetry breaking has also been taken into account (see supplementary information). The result favorably agrees with the observation. We note that STM measurements on epitaxially grown single layer graphene do not show this symmetry breaking. This is because the main graphene signal measured is near  $E_F$ , where no symmetry breaking is observed (see Fig. 4a).

In addition to these faint replicas, we observe additional intensity enhanced along the edge of certain medium sized hexagons around  $E_D$  (see gray broken and dotted lines in panel b). The origin of this intensity is still unclear. However, two observations can be made. 1) The center mid-sized hexagon around  $\Gamma$  (gray dotted lines) almost overlaps the first Brillouin zone of SiC. 2) All other hexagons (e.g. gray broken lines) are not regular, i.e. the six sides forming the hexagon do not have the same length. Interestingly, they all pass through K and K'. Whether this reveals the presence of perturbation that can hybridize the states at K and K' remains unclear.

In conclusion, we have reported the presence of an energy gap at the K point in epitaxial graphene and we propose that it is induced by the interaction with the substrate. Thus if one can change the strength of the interaction by changing the substrate on which graphene is grown, a control of the gap size can be possibly achieved. Since the epitaxial graphene is usually electron doped and the gap in this case is below  $E_F$ , the next important step to make graphene a semiconductor is to dope graphene with holes or to apply a gate voltage to move  $E_F$  inside the gap region.

## Methods

Atomically-thin graphene samples have been epitaxially grown by thermal decomposition of a Si-terminated n-type SiC wafer at increasing temperature [15, 20]. The details of the growth process and characterization of surface quality using low energy electron diffraction (LEED), and scanning electron microscopy (SEM) have been discussed elsewhere [15]. The thickness of the sample has been determined using Auger spectroscopy [20] and X-ray photoemission spectroscopy (XPS) [15] as well as ARPES. The absence of  $k_z$  dispersion in ARPES over a large momentum range of  $4\pi/c$  (see Fig. S1 in supplementary information) confirms the thickness of the single layer graphene.

ARPES data have been taken at Beamline 12.0.1 of the Advanced Light Source (ALS) in Lawrence Berkeley National Lab with photon energy of 50 eV (Figs.1 and 2 except Fig.2d) and Beamline 7.0.1 with photon energy of 140 eV (Fig.2d) and 100 eV (Fig.4). The energy resolution is 20-35 meV. The samples were measured at 25K with vacuum better than

$5.0 \times 10^{-11}$  Torr.

---

- [1] Novoselov, K.S., Geim, A.K., Morozov, S.V., Jiang, D., Zhang, Y., Dubonos, S.V., Grigorieva, I.V., Firsov, A.A. Electric field effect in atomically thin carbon films. *Science* **206**, 666-669 (2004).
- [2] Novoselov, K.S., Geim, A.K., Morozov, S.V., Jiang, D., Katsnelson, M.I., Grigorieva, I.V., Dubonos, S.V., and Firsov, A.A. Two-dimensional gas of Dirac fermions in graphene. *Nature* **438**, 197-200 (2005).
- [3] Zhang, Y.B., Tan, Y.-W., Stormer, H. L., and Kim, P. Experimental observation of the quantum Hall effect and Berry's phase in graphene. *Nature* **438**, 201-204 (2005).
- [4] Berger, C., Song, Z.M., Li, X.B., Wu, X.S., Brown, N., Naud, C., Mayou, D., Li, T.B., Hass, J., Marchenkov, A.N., Conrad, E.H., First, P.N., de Heer, W.A. Electronic confinement and coherence in patterned epitaxial graphene. *Science* **312**, 1191-1196 (2006).
- [5] Manes, J.L., Guinea, F. and Vozmediano, A.H. Existence and topological stability of Fermi points in multilayered graphene. *Phys. Rev. B* **75**, 155424 (2007).
- [6] Trauzettel, B., Bulaev, D.V., Loss, D. and Burkard, G. Spin qubits in graphene quantum dots. *Nature Phys.* **3**, 192-196 (2007).
- [7] Nakada, K., Fujita, M., Dresselhaus, G. and Dresselhaus M.S. Edge state in graphene ribbons: Nanometer size effect and edge shape dependence. *Phys. Rev. B* **54**, 17954-17961 (1996).
- [8] Brey, L., and Fertig, H.A. Electronic states of graphene nanoribbons studied with the Dirac equation. *Phys. Rev. B* **73**, 235411 (2006).
- [9] Son, Y.W., Cohen, M.L. and S.G. Louie. Energy gaps in graphene nanoribbons. *Phys. Rev. Lett.* **97**, 216803 (2006).
- [10] Han, M.Y., Ozyilmaz, B., Zhang, Y. and Kim, P. Energy band-gap engineering of graphene nanoribbons. *Phys. Rev. Lett.* **98**, 206805 (2007).
- [11] Nilsson, J., Castro Neto, A.H., Guinea, F and Peres, N.M.R. Transmission through a biased graphene bilayer barrier. <http://www.arxiv.org/abs/cond-mat/0607343> (2006).
- [12] During the long preparation of this manuscript, we became aware of this theoretical work: Giovannetti, G., Khomyakov, P.A., Brocks, G., Kelly, P.J. and van den Brink, J. Substrate-induced band gap in graphene on hexagonal boron nitride: Ab initio density functional cal-

- culations. *Phys. Rev. B* **76**, 073103 (2007).
- [13] McCann, E., and Fal'ko, V.I. Landau-level degeneracy and quantum Hall effect in a graphite bilayer. *Phys. Rev. Lett.* **96**, 086805 (2006).
  - [14] Ohta, T., Bostwick, A., Seyller, T., Horn, K., Rotenberg, E. Controlling the electronic structure of bilayer graphene. *Science* **313**, 951-954 (2006).
  - [15] Rollings, E., Gweon, G.-H., Zhou, S.Y., Mun, B.S., McChesney, J.L., Hussain, B.S, Fedorov, A.V., First, P.N., de Heer, W.A., Lanzara, A. Synthesis and characterization of atomically-thin graphite films on a silicon carbide substrate. *J. Phys. Chem. Solids* **67**, 2172-2177 (2006).
  - [16] Calandra M. and Mauri F. Electron-phonon coupling and electron self-energy in electron-doped graphene: calculation of angular resolved photoemission data. <http://www.arxiv.org/cond-mat/abs/0707.1467> (2007).
  - [17] Bostwick, A., Ohta, T., Seyller, T., Horn, K. and Rotenberg, E. Quasiparticle dynamics in graphene. *Nature Phys.* **3**, 36-40 (2006).
  - [18] Zhou, S.Y., Gweon, G.-H., Graf, J., Fedorov, A.V., Spataru, C.D., Diehl, R.D., Kopelevich, K., Lee, D.-H., Louie, Steven G., Lanzara, A. First direct observation of Dirac fermions in graphite. *Nature Phys.* **2**, 595-599 (2006).
  - [19] Zhou, S.Y., Gweon, G.-H., Lanzara, A. Low energy excitations in graphite: the role of dimensionality and lattice defects. *Annals of Physics* **321**, 1730-1746 (2006).
  - [20] Berger, C., Song, Z.M., Li, T.B., Li, X.B., Ogbazghi, A.Y., Feng, R., Dai, Z.T., Marchenkov, A.N., Conrad, E.H., First, P.N., de Heer, W.A. Ultrathin epitaxial graphite: 2D electron gas properties and a route toward graphene-based nanoelectronics. *J. Phys. Chem. B* **108**, 19912-19916 (2004).
  - [21] McClure, J.M. Band structure of graphite and de Haas-van Alphen effect. *Phys. Rev.* **108**, 612-618 (1957).
  - [22] Dresselhaus, M.S., and Dresselhaus, G. Intercalation compounds of graphite. *Adv. Phys.* **51**, 1-186 (2002).
  - [23] Guinea, F. Charge distribution and screening in layered graphene systems. Preprint at *Phys. Rev. B* **75**, 235433 (2007).
  - [24] Castro, E.V., Novoselov, K.S., Morozov, S.V., Peres, N.M.R., Lopes dos Santos J.M.B., Nilsson, J., Guinea, F., Geim, A.K., Castro Neto, A.H. Biased bilayer graphene: semiconductor with a gap tunable by electric field effect. <http://www.arxiv.org/abs/cond-mat/0611342>

- (2006).
- [25] Tsai, M.-H., Change, C.S. Dow, J.D., Tsong, I.S.T. Electronic contributions to scanning-tunneling-microscopy images of an annealed  $\beta$ -SiC(111) surface. *Phys. Rev. B* **45**, 1327-1332 (1992).
  - [26] Mallet, P., Varchon, F., Naud, C., Magaud, L., Berger, C., Veuillen, J.-Y. Electron states of mono- and bilayer graphene on SiC probed by STM. Preprint at <http://www.arxiv.org/abs/cond-mat/0702406> (2007).
  - [27] Rutter, G.M., Crain, J.N., Guisinger, N.P., Li, T., First, P.N., and Stroscio, J.A. Scattering and interference in epitaxial graphene. *Science* **317**, 219-222 (2007).
  - [28] Brar V., Zhang, Y.B., Yayan, Y., Ohta, T., McChesney, J., Horn, K., Rotenberg, E., Crommie, M. Scanning tunneling spectroscopy of inhomogeneous electronic structure in monolayer and bilayer graphene on SiC. Preprint at <http://www.arxiv.org/cond-mat/abs/0706.3764> (2007)
  - [29] Rutter, G. et al. APS March meeting, W29.00013 (2007).
  - [30] Hembacher, S., Giessibl, F. J., Mannhart, J., Quate C. F., Revealing the hidden atom in graphite by low-temperature atomic force microscopy. *Proc. Natl Acad. Sci. USA* **100**, 12539-12542 (2003).
  - [31] Varchon, F., Feng, R., Hass, J., Li, X., Nguyen, B.N., Naud, C., Mallet, P., Veuillen, U.Y., Berger, C., Conrad, E.H., Magaud, L. Electronic structure of epitaxial graphene layers on SiC: effect of the substrate. Preprint at <http://www.arxiv.org/abs/cond-mat/0702311> (2007).
  - [32] Emtsev, K.V., Seyller, Th. Speck, F., Ley, L., Stojanov, P., Riley, J.D., Lecker, R.G.C. Initial stages of the graphiteSiC(0001) interface formation studied by photoelectron spectroscopy. *Mater. Sci. Forum* **556-557**, 525 (2007).
  - [33] Shirley, Eric L., Terminello, L.J., Santoni, A. and Himpsel, F.J. Brillouin-zone-selection effects in graphite photoelectron angular distributions. *Phys. Rev. B* **51**, 13614-13622 (1995).

## Acknowledgments

We thank A. Geim and A.H. MacDonald for useful discussions, J. Graf for experimental assistance. This work was supported by the National Science Foundation through Grant No. DMR03-49361, the Director, Office of Science, Office of Basic Energy Sciences, Division of Materials Sciences and Engineering of the U.S Department of Energy under Contract

No. DEAC03-76SF00098, and by the Laboratory Directed Research and Development Program of Lawrence Berkeley National Laboratory under the Department of Energy Contract No. DE-AC02-05CH11231. A. H. C. N was supported through NSF grant DMR-0343790. S. Y. Zhou thanks the Advanced Light Source Fellowship for financial support.

Correspondence and requests for materials should be addressed to Alessandra Lanzara (Alanzara@lbl.gov).